THE INTERNATIONAL JOURNAL OF DEVELOPMENTAL BIOLOGY
www.intjdevbiol.com

Supplementary Material

corresponding to:

The *Hydra* FGF family – dispersed across the genome and expressed locally

KERSTIN OHLER, LISA REICHART, LARS KNEIFERT, SUSANNE ÖNEL, MONIKA HASSEL

Full Text for this paper is available at: https://doi.org/10.1387/ijdb.250118mh

S1A: NCBI and *Hydra AEP* Genome Project Portal sequence IDs of known (Lange et al., 2014) and new putative *Hydra vulgaris AEP* FGFs.

Hydra vulgaris AEP FGF	NCBI Sequence ID	*Hydra AEP* Genome Project Portal Sequence ID
FGFa	XP_047139867.1	HVAEP13.T024510.1
FGFb	XP_004209541.1	HVAEP3.T005481.1
FGFc	XP_065649609.1	HVAEP3.T006664.1
FGFe	XP_004206032.2	HVAEP3.T005247.2
FGFf	XP_012562921.1	HVAEP3.T006139.1
FGFg	XP_004206187.2	HVAEP12.T021850.1
FGFh	XP_047127889.1	HVAEP3.T006649.2
FGFi	XP_012560378.1	HVAEP3.T006662.1
FGFj	XP_002166704.4	HVAEP3.T006659.1
FGFk	XP_002165496.3	HVAEP12.T023185.1
FGFl	XP_004207236.2	HVAEP3.T006514.2
FGFm	XP_004207232.1	HVAEP3.T006522.1
FGFn	XP_012554564.1	HVAEP9.T016756.1
FGFo	XP_002170051.2	HVAEP12.T022802.3
FGFp	XP_047127904.1	HVAEP3.T006918.1

S1B: Physical features of *Hydra* FGFs. pI: Isoelectric point; GRAVY: Grand Average of Hydropathicity; kDa: kilodaltons.

Fibroblast growth factor	Molecular weight [kDa]	Positively charged residues	Negatively charged residues	Theoretical pI	GRAVY	Signal peptide likelihood
FGFa	18.6	21	19	8.3	-0.391	0
FGFb	22.7	31	16	9.8	-0.469	0.0265
FGFc	25.9	31	24	9.1	-0.661	0.5359
FGFe	25.6	31	15	10.0	-0.410	0.9351
FGFf	32.7	43	31	9.5	-0.640	0.9986
FGFg	27.2	36	24	9.5	-0.412	0.5854
FGFh	27.4	38	26	9.6	-0.556	0.9995
FGFi	24.0	27	15	9.6	-0.267	0.5317
FGFj	24.4	28	20	9.3	-0.252	0.3061
FGFk	26.8	31	29	8.1	-0.652	0
FGFl	26.6	41	24	10.0	-0.58	0.9996
FGFm	24.4	34	18	9.9	-0.311	0.9997
FGFn	21.9	30	23	9.1	-0.490	0.2876
FGFo	28.2	34	27	9.0	-0.382	0
FGFp	27.0	39	19	9.9	-0.536	0.6943

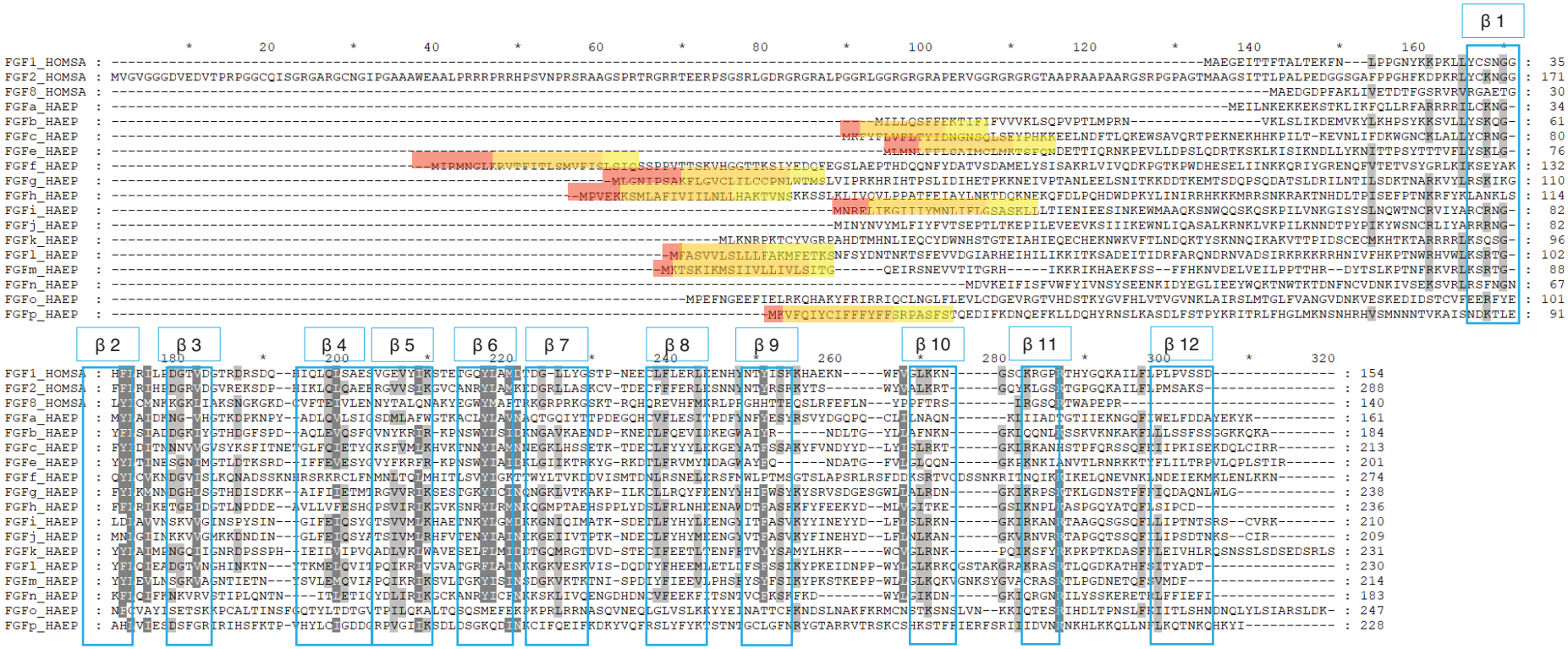

S2_1 Alignment: Amino acid alignment of *Hydra* AEP and *Homo sapiens* FGFs. Alignment calculated by ClustalX. Colour code for amino acids highlighted in the signal peptide: N-terminal region (red), central hydrophobic region (orange), C-terminal region (yellow). Blue frames show regions of antiparallel β-strands according to Mohammadi et al. (2005).

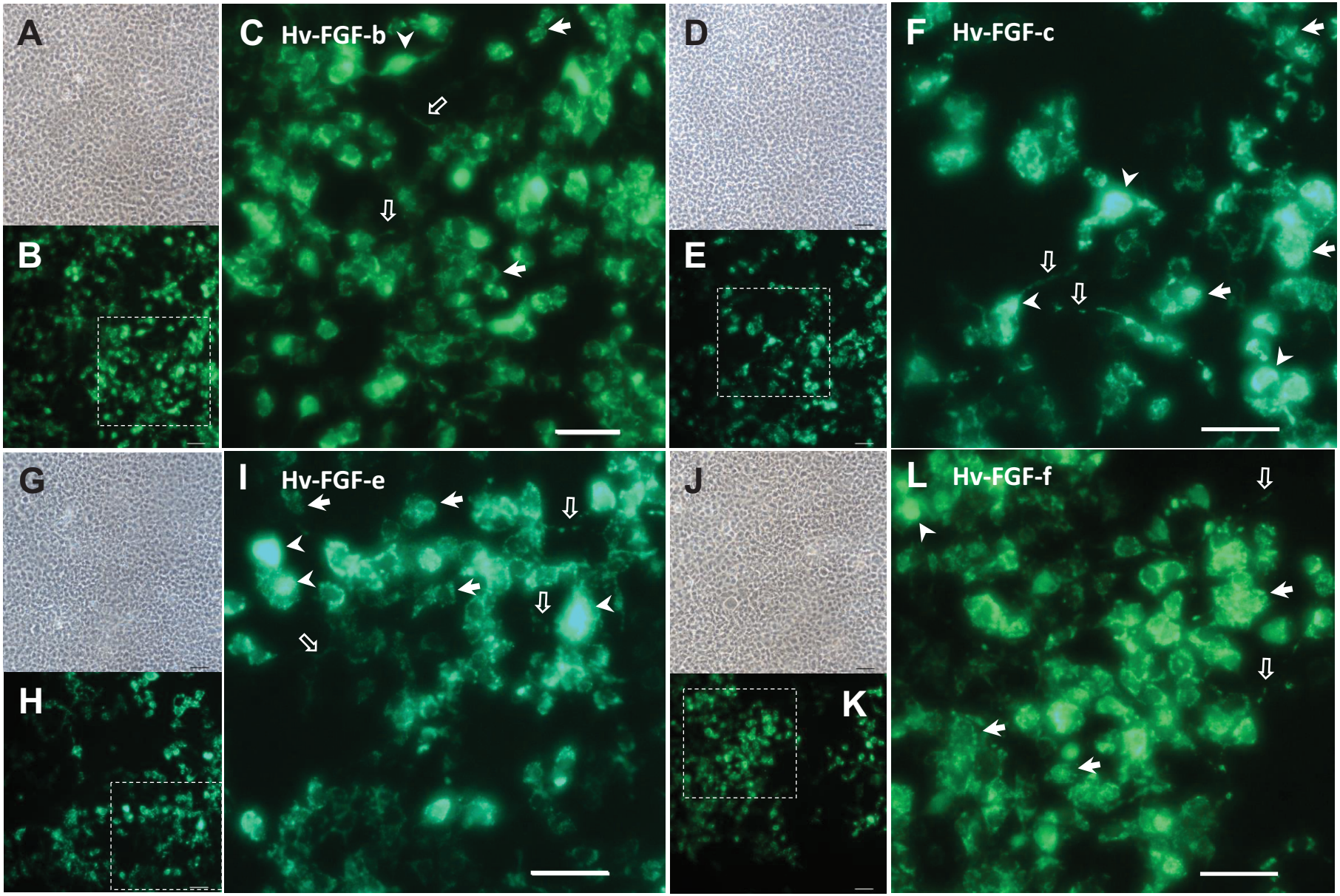

Fig. S2_2 Heterologous expression of myc-tagged *Hydra* FGFs in HEK293T cells. (A - C) Hv-FGF-b-myc, **(D – E)** Hv-FGF-c-myc, **(G - H)** Hv-FGF-e-myc, **(J – K)** Hv-FGF-f-myc. **(A, D, G, J)** light microscopy of the fixed, confluent cells. **(B, E, H, K)** Immunofluorescence of the same region following mouse anti-myc staining (detection using anti-mouse Alexa^{488}). **(C, F, I, L)** Enlarged regions as indicated to visualize staining of the whole cell (arrow heads), granular staining below the cell membrane (arrows) and filopodia / cytonemes (open arrows). Scale bar 50 μm

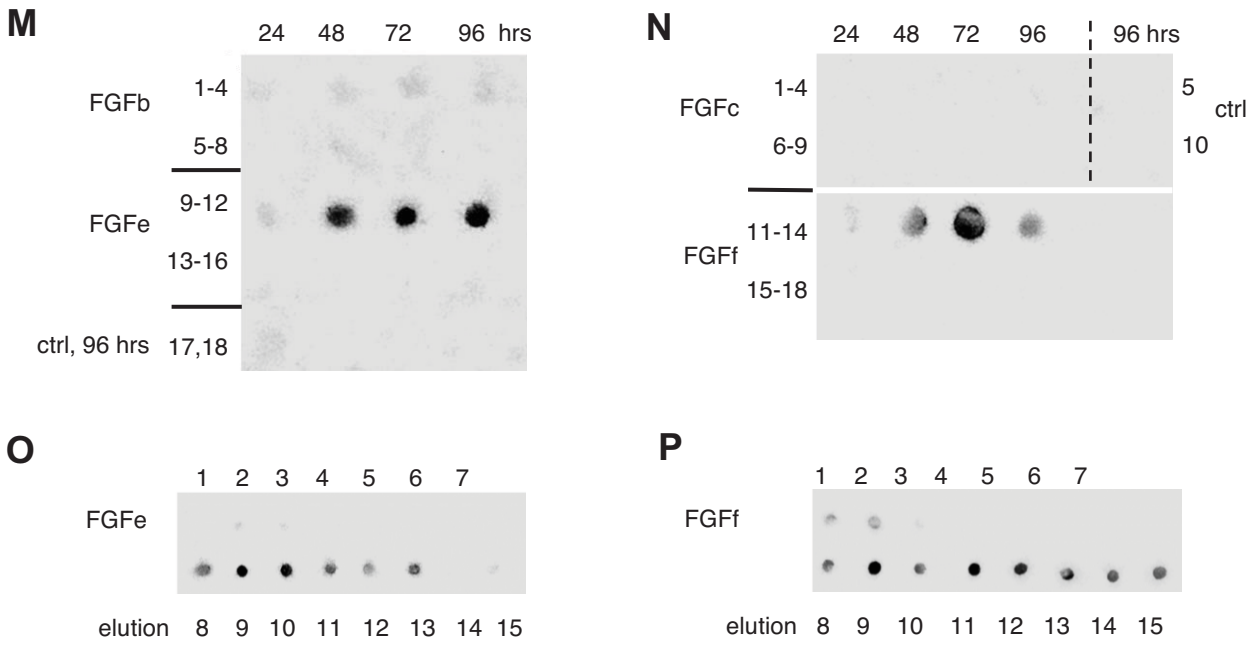

Fig. S2_3 Protein expression time series (Hv-FGF-b, Hv-FGF-c, Hv-FGF-e, Hv-FGF-f) and native purification of Hv-FGF-e and Hv-FGF-f by affinity chromatography.
(M-P) Dot blot images, visualization of the anti-myc antibody binding sites via ECL (2 min exposure). **(M)** 1-4: Hv-FGFb crude cell lysate, 5-8: Hv-FGFb medium. 9-12: Hv-FGFe crude cell lysate with FGFe detected between 48 and 96 hrs, 13-16: Hv-FGFe medium, 17: crude cell lysate of untransfected cells, 18: medium of untransfected cells at 96 hrs. **(N)** 1-4: Hv-FGFc crude cell lysate, 6-9: Hv-FGFc medium, 11-14: Hv-FGFf crude cell lysate with FGFf detected between 48 and 96 hrs, 15-18: Hv-FGF-f medium, 5: crude cell lysate of untransfected cells, 10: medium of untransfected cells. **(O, P)** Native purification of FGF-e **(O)** and FGF-f **(P)** using Ni-NTA affinity chromatography 1: crude cell extract, 2: cell lysate, 3-7: washing steps, 8-15: 1 ml elution steps; hpt: hours post transfection

S3_1_Summary of HydraT2T_AEP: FGF and FGFR(-like) genes on chromosomes 03, 09, 12 and 13

(features (blue) and ranges as provided by BLASTN and the Genome Data Viewer, https://www.ncbi.nlm.nih.gov/datasets/genome/GCF_037890685.1; 25.7.2025)

Chr.03, 70.902.961 nt

FGF-e HydraT2T_AEP, chr03
uncharacterized protein loc136077887
Range 1: 5.035.734 - 5.036.095
Range 2: 5.038.526 - 5038882
Range 3: 5.035.128 - 5035410
Range 4: 5.038.251 - 5038351

FGF-b HydraT2T_AEP, chr03
fibroblast growth factor 1
Range 1: 11.553.164 - 11.553.567
Range 2: 11.556.506 - 11556772
Range 3: 11.553.757 - 11553858

FGF-f HydraT2T_AEP, chr03
uncharacterized protein loc100213053 isoform x2
Range 1: 33.874.913 - 33.875.789
Range 2: 33.872.068 - 33872400
Range 3: 33.873.054 - 33873280
Range 4: 33.874.728 - 33874836
Range 5: 33.872.622 - 33872703

FGF-l HydraT2T_AEP, chr03
fibroblast growth factor 13 isoform x1
fibroblast growth factor 13 isoform x2
Range 1: 45.475.815 - 45.476.722
Range 2: 45.473.885 - 45474582
Range 3: 45.474.861 - 45.474.969

FGF-m HydraT2T_AEP, chr03
fibroblast growth factor 3
Range 1: 45.695.848 - 45696465
Range 2: 45.694.831 - 45695389
Range 3: 45.695.560 - 45695669

FGFR 45,822,834 - 45,831,958
FGFR-like 45,837,546 - 45,892,474

FGF-h HydraT2T_AEP, chr03
fibroblast growth factor 2
Range 1: 49,247,626 - 49,248,232
Range 2: 49,246,488 - 49,247,073
Range 3: 49,247,178 - 49,247,283

FGF-j HydraT2T_AEP, chr03
fibroblast growth factor 1
Range 1: 49.525.394 - 49525694
Range 2: 49.525.008 - 49525292
Range 3: 49.524.349 - 49524607
Range 4: 49.526.285 - 49.526.504
Range 5: 49.524.778 - 49524882

FGF-i HydraT2T_AEP, chr03
loc105846314, putative fibroblast growth factor 1
Range 1: 49.556.449 - 49556998
Range 2: 49.555.591 - 49555876
Range 3: 49.555.359 - 49555464
Range 4: 49.556.192 - 49556297

FGF-c HydraT2T_AEP, chr03
fibroblast growth factor 2 isoform x2
Range 1: 49.701.133 - 49.701.430
Range 2: 49.698.165 - 49.698.393
Range 3: 49.700.935 - 49.701.041

FGF-p HydraT2T_AEP, chr03
uncharacterized protein loc124808828 isoform x2
Range 1: 58.337.826 – 58338272
Range 2: 58.327.535 - 58327852
Range 3: 58.328.217 - 58328405

Chr.09, 65.083.506 nt

FGF-n HydraT2T_AEP, chr09
fibroblast growth factor 8
Range 1: 35.751.923 - 35752309
Range 2: 35.750.506 - 35750692
Range 3: 35.751.389 - 35751532
Range 4: 35.751.712 - 35751816
Range 5: 35.750.778 - 35750835

Chr.08, 69.605.405

FGF-c HydraT2T_AEP, chr08
fragment
18176 bp at 5' side:
uncharacterized protein loc136084282 isoform x2
20784 bp at 3' side:
uncharacterized protein loc124817691 isoform x2
Range 1: 30.761.768 - 30.761.990

BLASTN FGF-c-fragm. chr8 (410 nt)
The sequence corresponds 91% to a stretch of the 3' coding/3'UTR region of *Hv-fgf-c* cDNA (nt 992 – nt 1401), not predicted as a gene

Chr. 12, 86.977.266 nt

FGF-g HydraT2T_AEP, chr12
fibroblast growth factor 8
Range 1: 18.021.098 - 18021609
Range 2: 18.019.630 - 18019998
Range 3: 18.018.962 - 18019139
Range 4: 18.020.835 - 18020944

FGF-o HydraT2T_AEP, chr12
uncharacterized protein loc100200699 isoform x3
uncharacterized protein loc100200699 isoform x4
Range 1: 47.440.780 - 47441497
Range 2: 47.430.414 - 47430827
Range 3: 47.430.941 - 47431091
Range 4: 47.433.564 - 47433673

FGF-k HydraT2T_AEP, chr12
fibroblast growth factor 12 isoform x2
Range 1: 60.660.779 - 60661167
Range 2: 60.659.682 - 60659999
Range 3: 60.657.554 - 60657694
Range 4: 60.660.405 - 60660514

Chr.13, 61145.917 nt

FGF-a HydraT2T_AEP, chr13
low quality protein: chromodomain-helicase-dna-binding pr...fibroblast growth factor 6
Range 1: 17.776.933 - 17.777451
Range 2: 17.776.751 - 17.776.863

S3_2_ Summary of HydraT2T_105: FGF and FGFR(-like) genes on chromosomes 03, 09, 12 and 13

(features (blue) and ranges as provided by BLASTN / Genome Data Viewer, https://www.ncbi.nlm.nih.gov/datasets/genome/GCF_038396675.1; 25.7.2025)

Chr.03, 63.973.391 nt

FGF-e HydraT2T_105, chr03
uncharacterized protein loc101235893
Range 1: 5.285.842 - 5.286.199
Range 2: 5.282.496 - 5.282.854
7861 bp at 5' side: uncharacterized protein loc101235791381 bp at 3' side: uncharacterized protein loc101235893
Range 3: 5.281.902 - 5.282.182
uncharacterized protein loc101235893
Range 4: 5.285.537 - 5.285.637

FGF-b HydraT2T_105, chr03
fibroblast growth factor 1
1 Range 1: 11.665.478 - 11665881
3 Range 2: 11668792 - 11669058
Range 3: 11.666.081 - 11.666.182

FGF-f HydraT2T_105, chr03
uncharacterized protein loc100213053 isoform x1 uncharacterized protein loc100213053 isoform x1
Range 1: 30.619.735 - 30620614
Range 2: 30617099 - 30617437
Range 3: 30617916 - 30618134
Range 4: 30619550 - 30619658
Range 5: 30617657 - 30.617.730

FGF-l HydraT2T_105, chr03
fibroblast growth factor 13 isoform x1
fibroblast growth factor 13 isoform x2
Range 1: 41.251.003 - 41251909
Range 2: 41.248.465 - 41.249.160
Range 3: 41249440 - 41.249.548

FGF-m HydraT2T_105, chr03
fibroblast growth factor 3
Range 1: 41.424.154 - 41424712
Range 2: 41.425.185 - 41425794
Range 3: 41.424.900 - 41.425.003

FGFR 41,517,005..41,526,825
FGFR-like 41,536,156..41,549,495

FGF-h HydraT2T_105, chr03
fibroblast growth factor 1
Range 1: 43.977.533 - 43978108
Range 2: 43.976378 - 43976966
Range 3: 43.977.318 - 43.977.420

FGF-j HydraT2T_105, chr03
fibroblast growth factor 1
Range 1: 44.341.262 - 44341562
Range 2: 44.340.235 - 44340490
Range 3: 44.340877 - 44341164
Range 4: 44.342.134 - 44.342.354
Range 5: 44340649 - 44.340.753

FGF-i HydraT2T_105, chr03
putative fibroblast growth factor 1
Range 1: 44.365.355 - 44365873
Range 2: 44.364.370 - 44364655
Range 3: 44.364.958 - 44365063

FGF-c HydraT2T_105, chr03
uncharacterized protein loc101235368 isoform x1
Range 1: 44.447.773 - 44.448368
20948 bp at 5' side: uncharacterized protein loc1360925543109 bp at 3' side: uncharacterized protein loc101235368 isoform x1
Range 2: 44.442.744 - 44.443.285
uncharacterized protein loc101235368 isoform x1
Range 3: 44.446.598 - 44.446.889

FGF-p HydraT2T_105, chr03
uncharacterized protein loc124808828 isoform x1
Range 1: 51.475.139 - 51.475.579
Range 2: 51.459.376 - 51459693
Range 3: 51.460.057 - 51460245
Range 4: 51.459.783 - 51459902
Range 5: 51.473.077 - 51473127

Chr.09, 60.866.383 nt

FGF-n HydraT2T_105, chr09
fibroblast growth factor 8b
Range 1: 33.389.248 - 33389629
Range 2: 33.387.919 - 33388100
Range 3: 33.388788 - 33388931
Range 4: 33.389043 - 33389147

Chr. 12, 78.219.554 nt

FGF-g HydraT2T_105, chr12
fibroblast growth factor 17
Range 1: 15.923.888 - 15.924.399
Range 2: 15.922482 - 15922850
Range 3: 15.921.875 - 15922051
Range 4: 15.923619 - 15923728

FGF-o HydraT2T_105, chr12
ribonuclease h1 isoform x2
uncharacterized protein loc100200699 isoform x2
Range 1: 43.857.447 - 43858160
uncharacterized protein loc100200699 isoform x2
uncharacterized protein loc100200699 isoform x1
Range 2: 43.870.147 - 43870559
Range 3: 43.869.874 - 43870024
Range 4: 43.866.784 - 43866893

FGF-k HydraT2T_ 105, chr12
fibroblast growth factor 12 isoform x2
fibroblast growth factor 12 isoform x1
Range 1: 55.187.197 - 55187582
Range 2: 55.185.997 - 55186314
Range 3: 55.184.021 - 55184161

Chr.13, 54525.650 nt

FGF-a HydraT2T_105, chr13
chromodomain-helicase-dna-binding protein 1 isoform x2
chromodomain-helicase-dna-binding protein 1 isoform x1
Range 1: 13.465.661 - 13.466.176
Range 2: 13.465.478 - 13465590

Plate I

Supplement S4

Hv-fgf-a

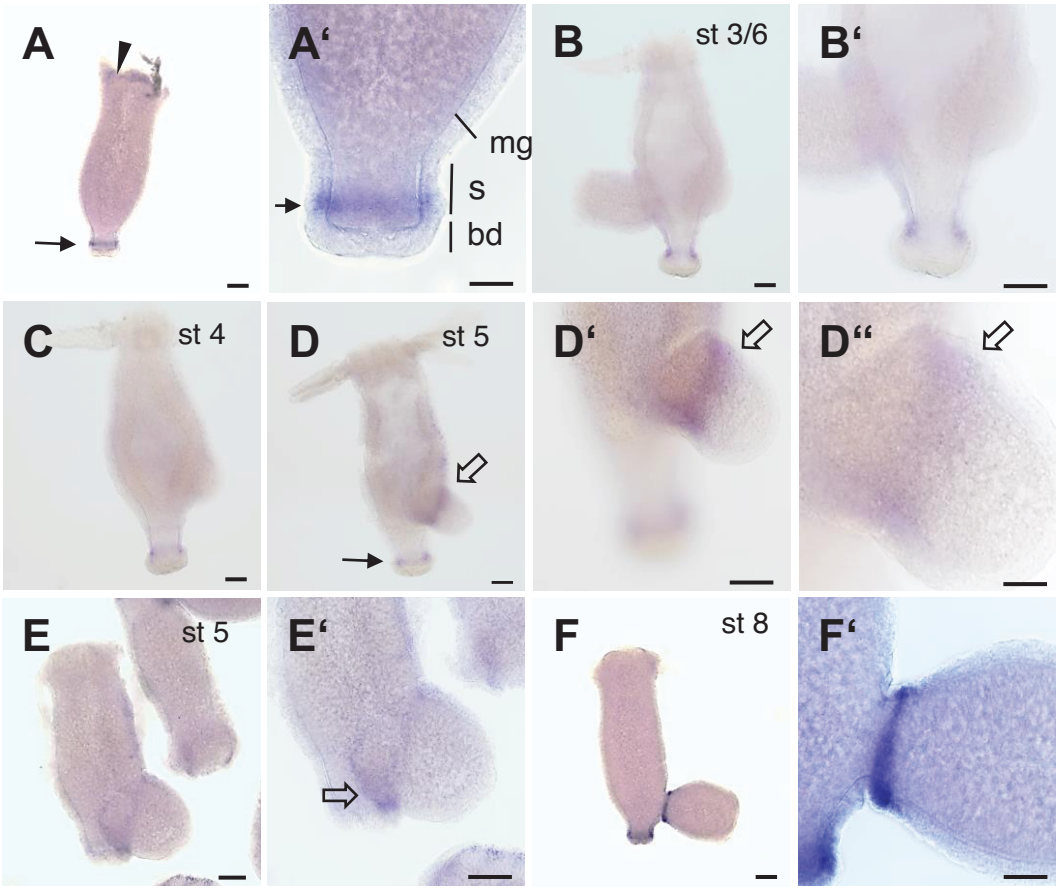

Hv-fgf-e

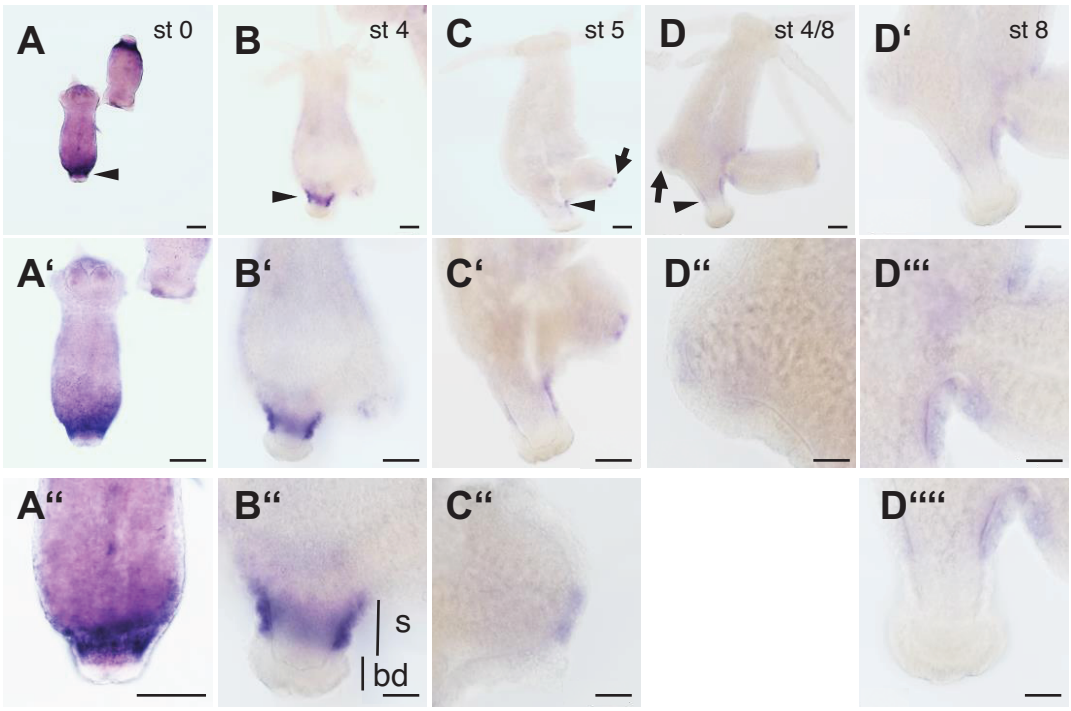

Supplement Figure S4, Plate I

Plate I *Hv-fgf-a:* Transcription in a ring above the basal disc

(A, A') *Hv-fgf-a wa*s upregulated in adult polyps in an ectodermal ring (arrow) of the proximal stalk (s), right above the basal disc (bd). The body column tissue (mainly the endoderm) was stained weakly and ubiquitous under these conditions. Animals became dark blue when stained > 1 hr with the pattern no longer recognizable. **(A)** Tentacle bases (arrowhead) were occasionally *Hv-fgf-a* -positive, but this expression domain was unreliable. **(B- B')** In the early bud evagination phase (stage 3, right bud) the gene was not expressed in bud tissue. **(B'** left bud, **C-E')** In the bud elongation phase (stages 4 and 5) *Hv-fgf-a* became upregulated in a broad zone comprising about 50% of the proximal bud tissue (open arrow). **(F, F')** The adult pattern established during the late budding process when the expression domain retracted towards the bud base until the basal constriction had formed in stage 8. This stage prepares the young polyp for detachment. From now on, the typical ectodermal ring of *Hv-fgf-a* positive cells - remote from the basal disc and proximal to the stalk region persisted. Dig-labelled *Hv-fgf-a* antisense RNA probe was diluted 1:20.000.

Plate I *Hv-fgf-e:* Transcription in a zone in the stalk above the basal disc

(A – B'') *Hv-fgf-e wa*s upregulated in adult polyps in the stalk ectoderm (arrow head) above the basal disc (bd) and - fading out towards the distal stalk (s) and budding zone. The body column ectodermal tissue stained weakly under these conditions, but animals became dark blue when stained > 1 hr (**A - A''** e.g. stained for 50 min instead of 30 min). **(A, A'; C – C'')** In some animals and developing buds, the circumference of the mouth opening (arrow in (C**))** was *Hv-fgf-e* positive about equally strong as the peduncle zone, but this pattern was not reproduced reliably. **(D-D'''')** The adult pattern established during the budding process from stage 8 onwards. Dig-labelled *Hv-FGFe* antisense RNA probe diluted 1:20.000.

Plate II

Supplement S4

Hv-fgf-f

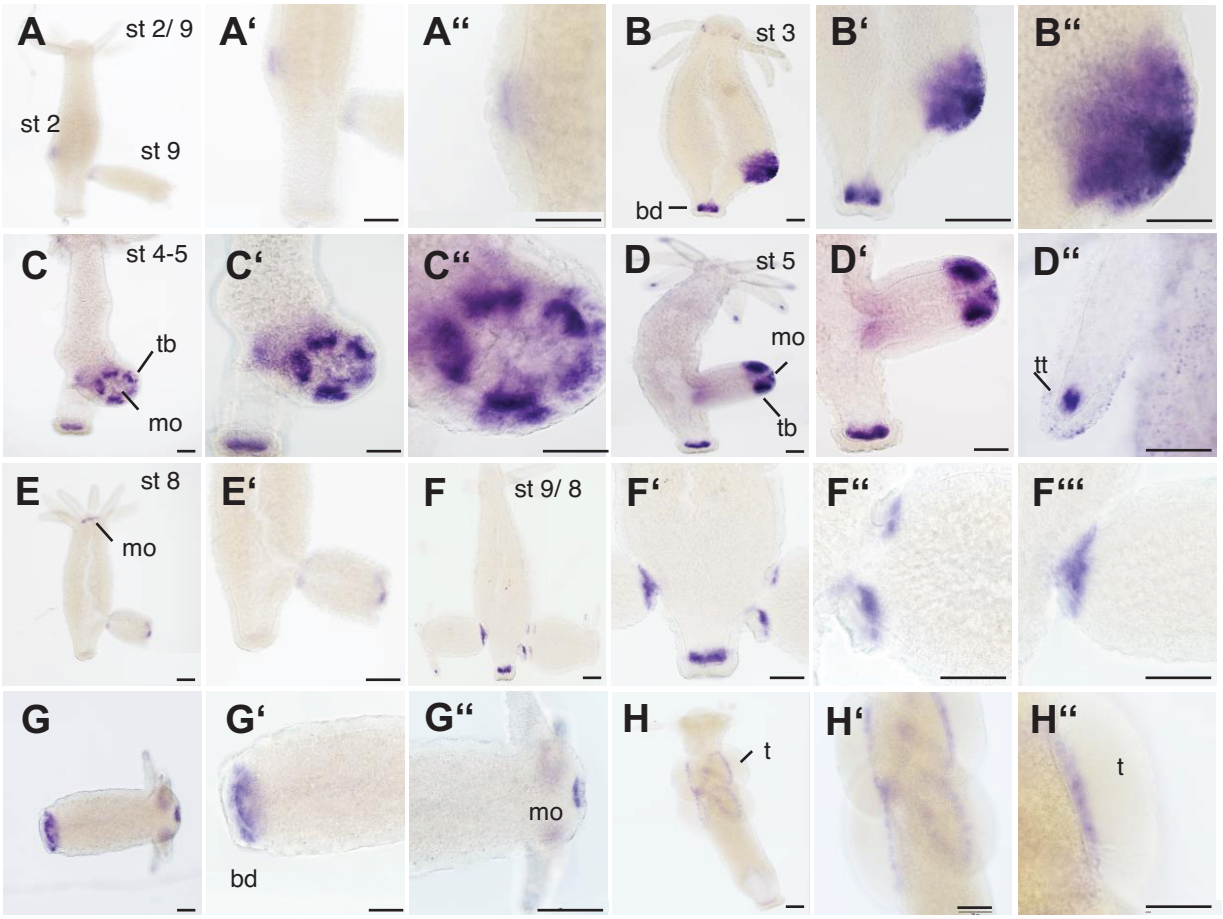

dISH

Hv-fgfr-a / Hv-fgfr-b

Hv-fgfr-a / Hv-fgf-f

Hv-fgfr-b / Hv-fgf-f

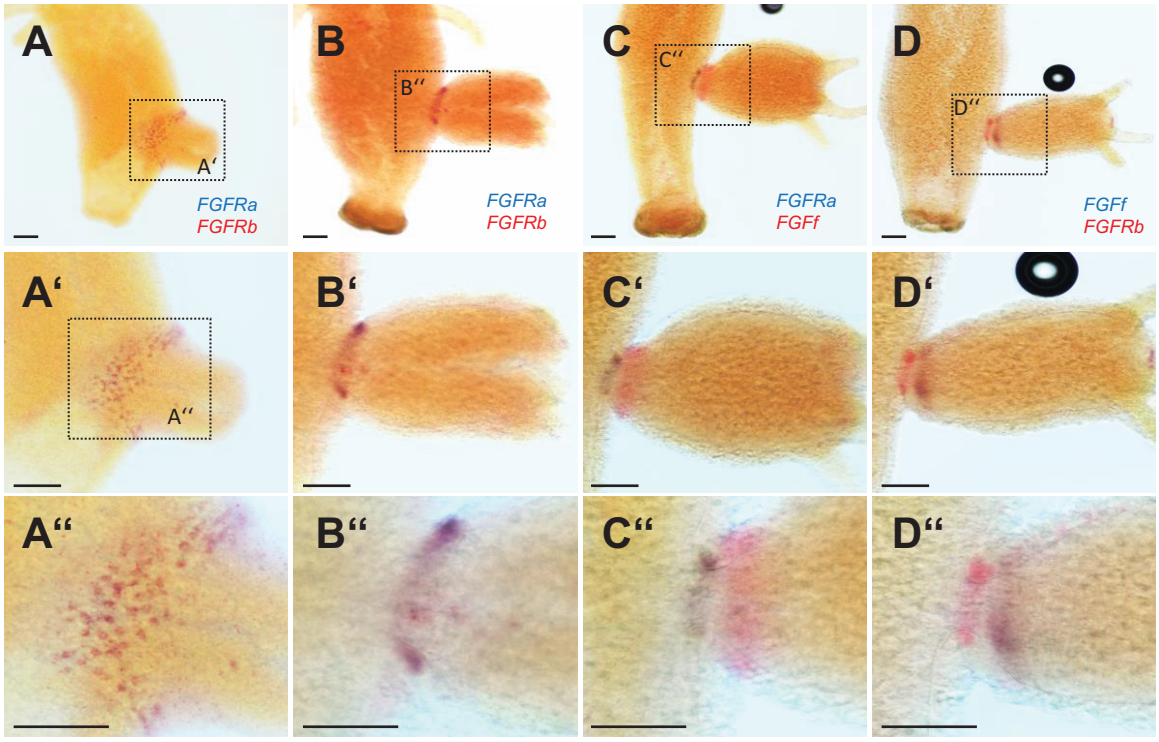

Supplement Figure S4, Plate II, III and IV

Plate II *Hv -fgf-f*: Transcription in developing buds, their tentacle zone and base

The Hv-fgf-f expression pattern has been described in (Lange et al., 2014) already. We here show some more details. **(A – A'')** The gene marks the early bud endoderm in stage 2 stronger than the basal disc which is always *Hv-fgf-f* - positive. **(B – B'')** *In s*tage 3 buds, a strong ectodermal and central expression has developed in the evaginating bud and particularly the bud tip – from which later tentacles and mouth opening will form. **(C- C'')** The prospective tentacle bud ectoderm (tb) region is *Hv-fgf-f* – positive from stage 4-5 onwards (elongation phase of the bud), although tentacle buds are not yet visible. **(D - D')** In a lateral view, it becomes obvious that the ectodermal mouth opening (mo) is surrounded by a few *Hv-fgf-f* - positive cells. **(D'')** The adult tentacle tip (tt) expresses the gene endodermal, just like the basal disc. **(E – E')** *Hv-fgf-f* mRNA level is higher in the tentacle and mouth zone than the basal disc expression domain as assessed by allowing a shorter colour development. **(F – F'')** In the bud constriction and detachment phase, the basal disc endoderm expresses *Hv-fgf-f* strongly. **(G – G'')** The detached bud transcribes the gene in the basal disc endoderm, in the ectoderm surrounding the mouth and in the tentacle tips and bases, however weaker in the latter than around the mouth. **(H – H''')** In sexual animals carrying testes, *Hv-fgf-f* is expressed in cells at the base of developing testes (t). Dig-labelled antisense probe diluted 1:2000.

Plate II dISH: Double in situ hybridization in combinations of the two *Hv-FGFR*s and *Hv-FGFf*. The respective combination is indicated in panels A-D. **(A-A'', B-B'')** Transcription domains of the two FGFRs overlap completely (purple). (**C-C'', D-D'**'') *Hv-FGFR-a* or *Hv-FGFR-b* and *Hv-FGF-f* are expressed adjacent to each other with the *Hv-FGF* being expressed in the bud and Hv-FGFR in the parent tissue. Method according to Hansen et al., 2000. Digoxigenin-labelled RNA probes were used as 1:2000 to 1:20.000 dilutions and stained with Fast red (red), fluorescein-labelled probes were used 1:1000 diluted and stained with NBT/BCIP (blue).

Plate III Expression patterns of the newly identified *Hv-fgf-g, Hv -fgf-h, Hv -fgf-i, Hv -fgf-j, Hv -fgf-k and Hv -fgf-l.* (A-C) *Hv-fgf-g* is expressed in the basal disc endoderm only (18/21). **(D-E') *Hv -fgf-h*** transcription is weak in the endoderm. **(D)** The gene is upregulated in early testis ubiquitously (19/22) and in late testis restricted to the distalmost cells (4/6, arrow). **(F-H) *Hv-fgf-i*** is upregulated in the tentacle tip ectoderm only (7/7) and weakly in early testes (3/7). **(I-I') *Hv-fgf-j*** mRNA is restricted to the tentacle tip endoderm (4/5). **(J-L''') *Hv -fgf-k*** mRNA was detected weakly in the whole endoderm (15/15) and upregulated in a zone between the tentacle bases (15/15) **(J, K, K')** as well as strongly in testes (12/12) **(J, J', K, L-L''')** plus and in a weaky expressing ring of cells above the basal disc (12/13, arrows in **J', J'', K',** depict these three regions). (**N-P'') *Hv -fgf-l*** showed a complex expression pattern with **(N, N'', O'', P'')** upregulation in a tightly restricted endodermal ring of the upper basal disc (16/16) and **(M, O, O')** strong expression in concentric zones surrounding the bud tip in early evaginating buds (5/5). **(N, N', P-P')** The gene is an early ectodermal marker for tentacle positions while no tentacle buds are visible yet (arrow) and for the mouth opening. **(N')** It seems to demark a broad tissue region (still fused?), from which two tentacles might sprout (open arrowheads). *In situ* hybridization of *Hv-fgf-n* was not successful.

Plate III

Supplement S4

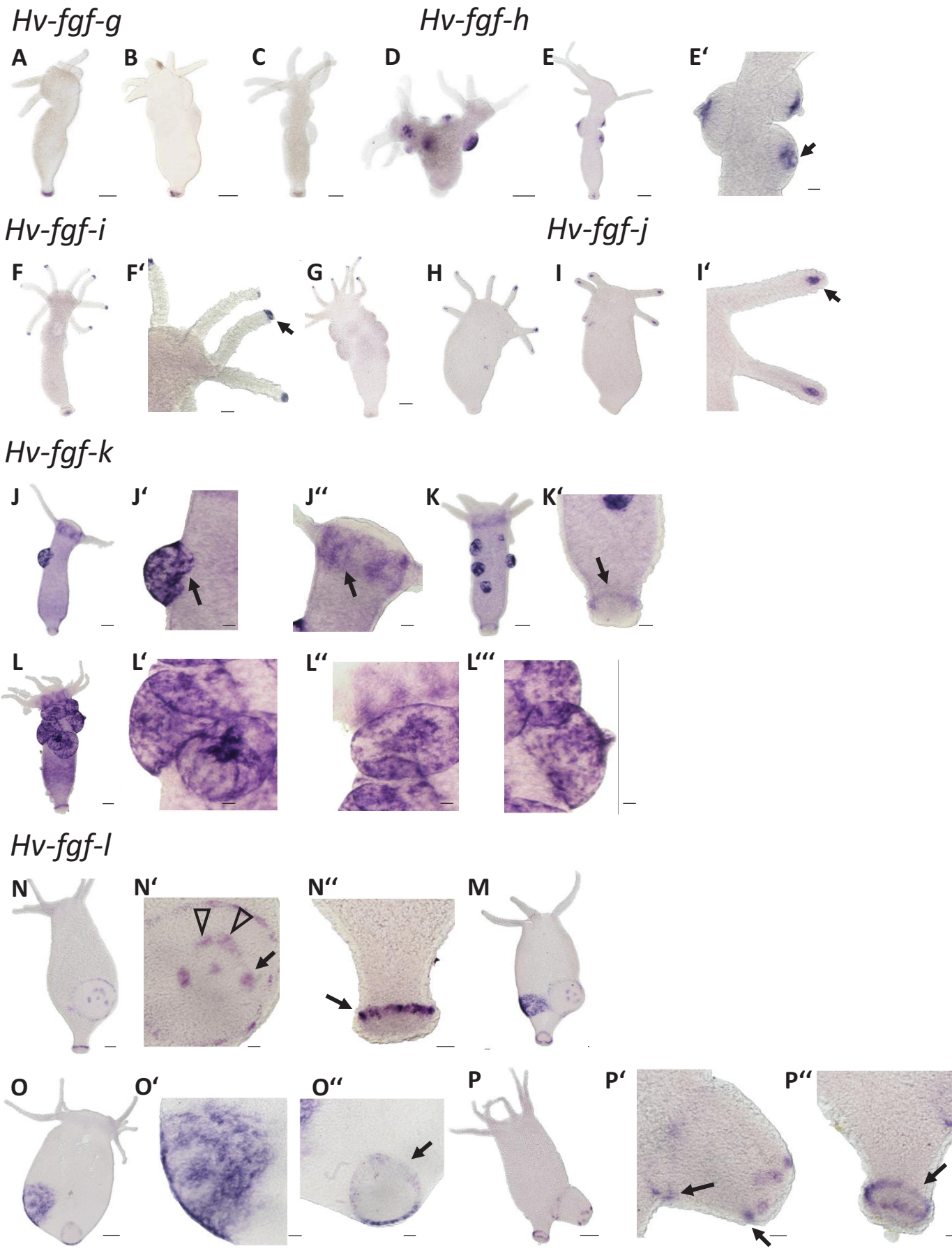

Plate IV

Hv-fgf-m

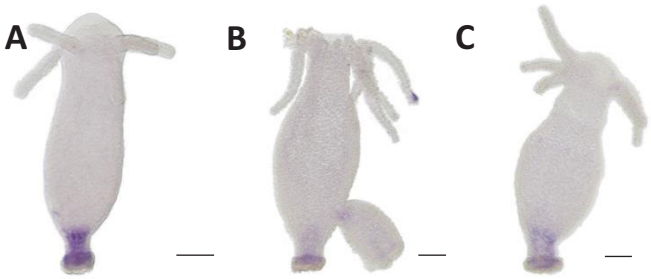

Hv-fgf-o *Hv-fgf-p*

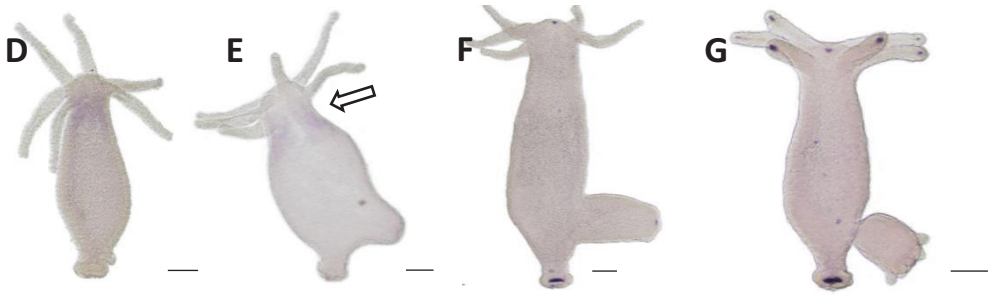

Plate IV Expression patterns of *Hv -fgf-m, Hv-fgf-o, Hv -fgf-p.* **(A-C)** *Hv -fgf-m* was detected in the whole basal disc and stalk endoderm (19/19). **(D-E) *Hv-fgf-o*** mRNA was found weakly expressed (but consistent), in the neck region between tentacles and the bulging gastric region (11/17, open arrow). **(F, G) *Hv-fgf-p*** was detected in a few cells of the endoderm surrounding the mouth opening (5/6) and in the basal disc (4/4) as well as sporadically in tentacle tips (1/4).

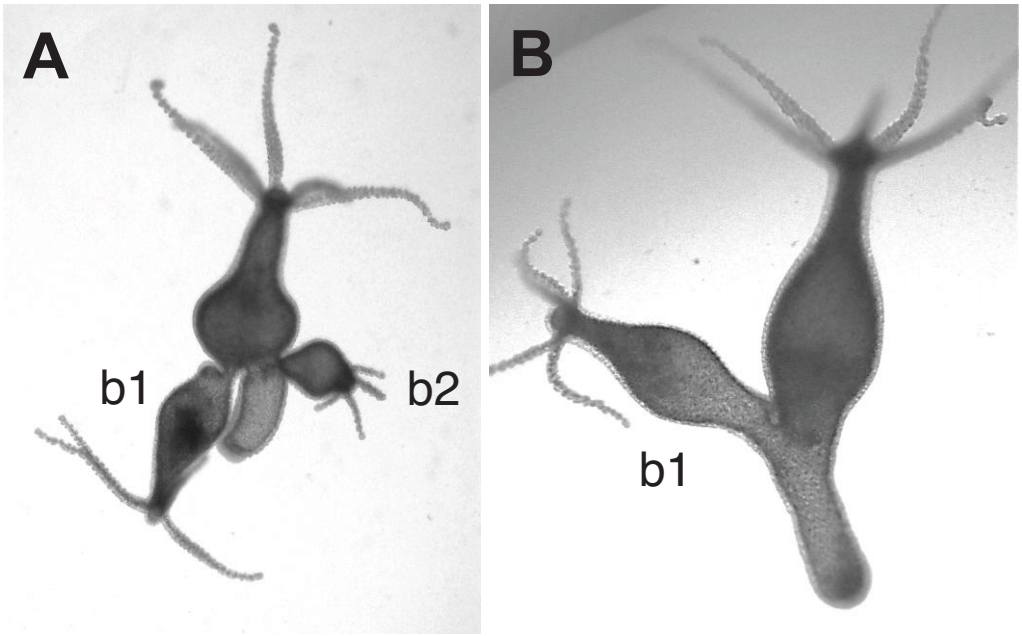

Evaluation of double axes obtained in two independent sets of triplicate siRNA for *fgfr-a_1*

	siRNA	Survival rate	Double axis non-detaching buds	Additional double axis
Experiment 1	*fgfr-a_1*	94,3 % (33/35)	51,5 % (17/33)	-
	pGL2	94,3 % (33/35)	0 % (0/33)	9,1 % (3/33)
Experiment 2	*fgfr-a_1*	96,7 % (29/30)	58,6 % (17/29)	-
	pGL2	90 % (27/30)	10,3% (3/27)	7,4 % (2/27)

S5_1: Results of siRNA electroporation with *FGFR-a* (positive control) and *pGL2* (negative control). The table summarises data of two experiments with triplicates. (A, B) Typical branched phenotypes obtained following electroporation with 3 micromolar *Hv-fgfr-a_1* siRNA on budding polyps carrying a stage 3 bud. The term additional double axis refers to double axes occurring as a split head outside the budding region. Such animals were observed with *pGL2* siRNA only. Evaluation on day 14 post electroporation. b1 bud resulting from the bud electroporated in stage 3 with the siRNA, b2 secondary bud formed on day 7 after the electroporation. These buds are able to detach, but detachment takes much longer than usual (up to 10 days instead of 4 days).

S5_2 Raw data of siRNA electroporation experiments with *Hv-fgf-b, Hv-FGF-c, Hv-fgfr-a* and *scrGFP* - evaluating nodular tentacles

date of eval	siRNA	N =	animals with nodules =	% phenotypes
22.07.2024	fgf-c_1	13	7	54%
22.07.2024	fgf-c_1	13	6	46%
22.07.2024	fgf-c_2	10	4	40%
22.07.2024	fgf-c_2	10	5	50%
24.07.2024	fgf-c_1	10	7	70%
24.07.2024	fgf-c_2	10	4	40%
	sum fgf-c	66	33/66	50%
mean fgfc1		6,67		
mean fgfc2		4,33		
mean fgf-c		5,50		
standard deviation fgf-c			1,26	
standard deviation fgf-c-1			0,47	
standard deviation fgf-c-2			0,47	
22.07.2024	fgf-b_1	11	0	
22.07.2024	fgf-b_1	11	0	
22.07.2024	fgf-b_2	11	0	
22.07.2024	fgf-b_2	10	0	
24.07.2024	fgf-b_1	10	0	
24.07.2024	fgf-b_2	10	0	
	sum fgf-b	63	0/63	
mean fgf-b_1		11,00		
mean fgf-b_2		10,00		
22.07.2024	scrGFP	10	0	
22.07.2024	scrGFP	10	0	
24.07.2024	scrGFP	10	0	
	sum scrGFP	30	0/30	
mean ScrGFP		10,00		
22.07.2024	fgfr-a	10	0	
22.07.2024	fgfr-a	10	0	
24.07.2024	fgfr-a	10	0	
	sum fgfr-a	30	0/30	
mean fgfr-a		10,00		

S5_2 Raw data of siRNA electroporation experiments with *Hv-fgf-b, Hv-FGF-c, Hv-fgfr-a* and *scrGFP* - evaluating nodular tentacles

date of eval	siRNA	N =	animals with nodules =	% phenotypes
22.07.2024	fgf-c_1	13	7	54%
22.07.2024	fgf-c_1	13	6	46%
22.07.2024	fgf-c_2	10	4	40%
22.07.2024	fgf-c_2	10	5	50%
24.07.2024	fgf-c_1	10	7	70%
24.07.2024	fgf-c_2	10	4	40%
	sum fgf-c	66	33/66	50%
mean fgfc1		6,67		
mean fgfc2		4,33		
mean fgf-c		5,50		
standard deviation fgf-c			1,26	
standard deviation fgf-c-1			0,47	
standard deviation fgf-c-2			0,47	
22.07.2024	fgf-b_1	11	0	
22.07.2024	fgf-b_1	11	0	
22.07.2024	fgf-b_2	11	0	
22.07.2024	fgf-b_2	10	0	
24.07.2024	fgf-b_1	10	0	
24.07.2024	fgf-b_2	10	0	
	sum fgf-b	63	0/63	
mean fgf-b_1		11,00		
mean fgf-b_2		10,00		
22.07.2024	scrGFP	10	0	
22.07.2024	scrGFP	10	0	
24.07.2024	scrGFP	10	0	
	sum scrGFP	30	0/30	
mean ScrGFP		10,00		
22.07.2024	fgfr-a	10	0	
22.07.2024	fgfr-a	10	0	
24.07.2024	fgfr-a	10	0	
	sum fgfr-a	30	0/30	
mean fgfr-a		10,00		

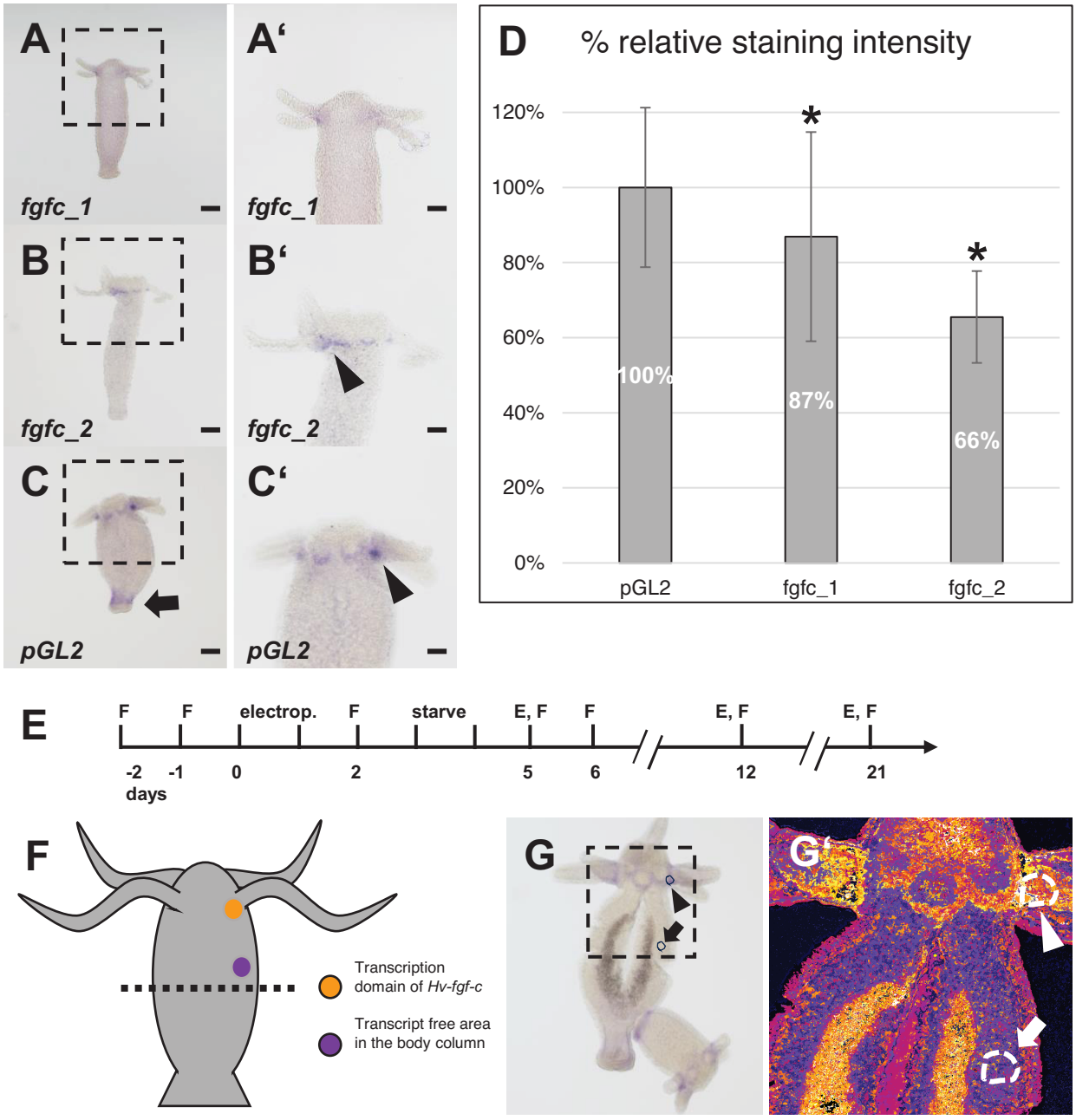

Fig. S6 siRNA controls and evaluation of knockdown. *Hv-fgf-c* expression patterns and relative staining intensity (mRNA expression) after siRNA-mediated knockdown five days post electroporation. (A, A‘) *siFGFc_1* knockdown diminished the *Hv-fgf-c* mRNA expression in tentacles (>80%). (B, B‘) siFGFc_2 knockdown only partially reduced the FGFc gene expression (~ 50%). Both siRNAs completely removed expression in the stalk. (C, C‘) Control pGL2 does not affect *Hv-fgf-c expression,* the characteristic FGFc transcription below the tentacles (arrowheads) and in the stalk persist (arrows). (D) Knockdown efficiency of *Hv-fgf-c* given as percentage of the relative staining intensity of *fgf-c* in controls. Asterisks (*) denote statistical significance at 5% (p-value ≤ 0.05). F feeding/washing, E evaluation. (E) Timeline of the siRNA experiments. (F - G‘) Determination of *Hv-fgf-c* mRNA expression intensity using the Mean Gray Value (MGV). (F) Scheme of a *Hydra* polyp depicting the standardized measuring areas for the MGV. (G, G’) Adult *Hydra* control polyp with the *Hv-fgf-c* mRNA expression pattern. Measurement was in two defined areas: (1) at the tentacle base (arrow head) and (2) in the expression-free body (arrow). The relative expression intensity of *Hv-fgf-c* mRNA was calculated with the MGV. The dark brown staining in the broken body column is an artefact. Scale bar 100 µm